Dielectric Relaxation Due to Impurity-Vacancy Complexes in NaCl Crystals*

R. W. DREYFUS
International Business Machines Research Center, Yorktown Heights, New York
(Received September 19, 1960; revised manuscript received December 5, 1960)

Sodium-ion vacancies are introduced into sodium chloride crystals by the addition of the following divalent cation impurities: Mg^{++}, Mn^{++}, Ca^{++}, Zn^{++}, Cd^{++}, and Sr^{++}. Below 150°C, the virtual negative charge of a cation vacancy binds the majority of the vacancies to the divalent impurity ions to form complexes. The reorientation of these dipolar complexes is observed in the present experiments as a transient dielectric polarization current occurring immediately after the application of a dc electric field. Below 0°C, the dominant effect is an exponential "fast polarization" due to complexes in which the vacancy is in the nearest sodium-ion site to the impurity ion (except for the case of NaCl:Mg^{++}). Also observed is a "very fast polarization" which may be interpreted as due to next-nearest-neighbor impurity-vacancy complexes, plus a "slow polarization" ascribed to vacancies jumping between more distant bound sites. By combining the present measurements with earlier ac measurements, one can obtain particularly accurate values for the jump activation energies of vacancies occupying the nearest-neighbor site to Ca^{++} and Mn^{++} ions in a NaCl crystal. The energies obtained for these two cases are 0.702±0.010 ev and 0.680±0.010 ev, respectively. From the manner in which the relaxation time at a given temperature varies with the radius of the impurity ion, the dominant jump mechanisms can be inferred. The major reason for the decrease in relaxation time with decreasing radius of the impurity ion appears to be the strong dependence of the jump rate of the impurity ion on ionic radius.

I. INTRODUCTION

IONIC conductivity in the alkali halides is known to take place through the migration of free positive-ion vacancies in an electric field.[1] It is further established[2] that divalent cation impurities added to an alkali halide crystal enter the lattice substitutionally; to maintain the electrical neutrality of the crystal then requires the simultaneous creation of an equal number of positive-ion vacancies. In this way the electrical conductivity can be considerably enhanced. A summary of the many investigations dealing with the ionic conductivity of doped alkali halide crystals is given by Lidiard.[1] In addition to the enhancement of the free positive-ion vacancies in crystals by the addition of divalent impurities, there is also, in the lower temperature range, the formation of impurity-vacancy complexes. These complexes result from the electrostatic attraction that exists between the excess positive charge of the impurity ion and the virtual negative charge of the cation vacancy. In sodium chloride, such impurity-vacancy complexes are bound with an energy of 0.35 to 0.50 ev.[3] Below a temperature of about 200°C, the majority of the vacancies are in this bound state (usually referred to as "associated").

When the divalent impurity ion is in the (0,0,0) lattice site, a complex may be formed in which the vacancy occupies a nearest-neighbor (n.n.) sodium-ion site, of the type $(\frac{1}{2},\frac{1}{2},0)$, or a next nearest-neighbor (n.n.n.) sodium-ion site[4] of the type (1,0,0). The n.n. and n.n.n. sites are located at distances $\sqrt{2}a$ and $2a$, respectively, from the impurity ion, where a is the sodium-chlorine spacing. At relatively low temperatures, occupancy of more distant sites than these is improbable because of the Coulomb attraction between the vacancy and impurity which makes the potential energy increase rapidly with distance. On the other hand, detailed calculations indicate that the binding energies of the n.n. and n.n.n. sites are nearly equal.[5] In the case of the n.n. vacancy, the increased Coulomb energy tends to be compensated for by the fact that the immediate lattice does not appear as a homogeneous dielectric medium. The absence of a polarizable Cl^- ion between the impurity and the n.n. vacancy reduces the binding energy to about the same as the n.n.n. site. The size of the impurity ion actually determines whether the n.n. or n.n.n. site is the more stable, since the positions of the nearest Cl^- ions depend on the radius of the impurity ion.

Since the impurity-vacancy complex is an electric dipole, with the vacancy end negative and the impurity end positive, its energy depends upon its orientation with respect to an applied electric field. Consequently, the application of an electric field will result in a preferential reorientation of these complexes, in the manner shown in Fig. 1. When an ac electric field is applied, the continual striving of the complexes to readjust their orientations to an equilibrium value consistent with the instantaneous applied field, produces an alternating current which lags in phase behind the field. This phenomenon is most conveniently measured as a dielectric loss, which is anticipated to obey the well-known Debye equations.[6] Such loss peaks have been observed in doped alkali halide crystals,[7–9] but are usually found to be somewhat broader than a Debye

* Part of a dissertation presented for the degree of Doctor of Philosophy at Yale University.

[1] A. B. Lidiard, in *Handbuch der Physik*, edited by S. Flügge (Springer-Verlag, Berlin, 1957), Vol. 20, p. 246.

[2] H. Pick and H. Weber, Z. Physik **128**, 409 (1950).

[3] F. Bassani and F. Fumi, Nuovo cimento **11**, 274 (1954).

[4] Since motion of the chlorine ions does not enter directly into the polarization, the terminology "n.n." and "n.n.n." will refer only to sodium-ion positions.

[5] M. Tosi and G. Airoldi, Nuovo cimento **8**, 584 (1958).

[6] P. Debye, *Polar Molecules* (The Chemical Catalog Company, Inc., New York, 1929), Chap. V, p. 77.

[7] Y. Haven, J. Chem. Phys. **21**, 171 (1953).

[8] J. Dryden and R. Meakins, Discussions Faraday Soc. **23**, 39 (1957).

[9] G. D. Watkins, Phys. Rev. **113**, 91 (1959).

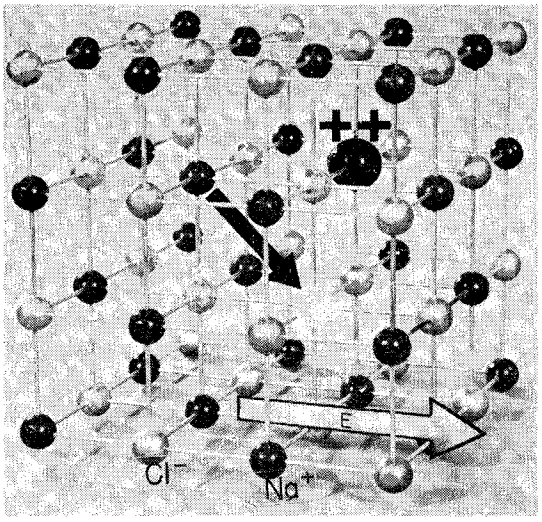

FIG. 1. Model of a lattice in which a vacancy (in white) is the nearest neighbor (n.n.) of a doubly charged metallic impurity ion. The interchange of an n.n. sodium ion with the n.n. vacancy, which would be favored by the applied electric field, **E**, is shown.

peak. In attempting to explain this broadening, Lidiard[10] has considered the effect of vacancies occupying n.n.n. sites. Lidiard's solution, for an ac applied field, shows the dielectric loss peak to be broader than a Debye peak. This solution is difficult to use, since the separation of the n.n. contribution from the higher order relaxation is not evident.

A second technique for detecting preferential reorientation of complexes, not hitherto utilized, is in the measurement of the transient polarization current flowing after the application of a dc field. In the presence of a static dc field, the impurity end of the impurity-vacancy complex tends to be oriented toward the field direction as is suggested by Fig. 1. The distribution of orientations will approach an equilibrium state, thereby producing a polarization current which decreases with time.

The present work was performed in the hope that the improved resolution available by the use of dc techniques at low temperatures would allow the separation of the n.n. relaxation from higher order relaxations. In addition, the impurity radius is treated as a variable by doping with different divalent cations having a wide range of ionic sizes. In this way, the variation of jump frequencies as well as the relative occupation of the n.n. and the more distant sites can be studied as a function of the radius of the impurity ion.

II. SAMPLE PREPARATION

The "lab-grown" crystals were prepared from the melt by a method similar to that described by Kremers.[11] A conical platinum crucible was lowered through a temperature gradient of 50°C/cm. After complete solidification, the crucible was inverted and a brief heating at 850°C was sufficient to release the crystal from the crucible. The crystal was then cooled slowly to room temperature. The average ingot weighed 100 g. Crystals of dimensions approximately 2×2×0.4 cm were usually obtained from regions of good cleavage in the lower third of the ingot.

The starting material was reagent grade sodium chloride. Some crystals were grown in nominally "pure" condition, but usually Mg, Zn, Mn, Cd, Ca, or Sr were added in the form of the chloride.

In addition to the lab-grown materials, measurements were also made on crystals obtained from the Harshaw Chemical Company. Doped crystals containing zinc and magnesium were also prepared by diffusing the impurity into Harshaw crystals. For this purpose, faces of 1×1×0.15 cm plates were covered with a thin coat of zinc or magnesium chloride, and the samples were annealed at 30°C below the melting point for a period of 72 hours. The outer 0.5 mm was then cleaved from each face. The second column of Table I indicates the method of preparation used for each sample studied.

Impurity precipitation was minimized by reheating and rapidly cooling the sodium chloride samples. For this purpose the 2×2×0.4 cm slabs obtained from the melt-grown crystals were heated to 350°C for 30 min in air. The slabs were then withdrawn from the furnace, air-cooled to room temperature, and samples of approximate dimensions 1×1×0.04 cm were then cleaved. Polarization measurements were usually completed within four days after this treatment. The as-received Harshaw crystal, however, was not reheated.

Electrodes of graphite or silver paint[12] were applied

TABLE I. Metallic impurities present in NaCl samples.

Impurity (ionic radius in A)	Sample[a]	Impurity conc. (ppm)	Rejection ratio (melt:solid)
Mg (0.65)	*L* 67	18±5	17:1
Mg (0.65)	*L* 70	580±180	17:1
Mg (0.65)	*D* 1	725±140	···
Zn (0.74)	*L* 68	50±20	60:1
Zn (0.74)	*L* 69	50±20	60:1
Zn (0.74)	*D* 3	~300	···
Mn (0.80)	*L* 33*A*	~200	···
Mn (0.80)	*L* 33*B*	200±8	15:1
Mn (0.80)	*L* 33*C*	~200	···
Cd (0.97)	*L* 40	770±160	3.9:1
Ca (0.99)	*L* 64	2600±400	1.2:1
Sr (1.13)	*L* 66	86±49	1.2:1
Harshaw	*H* 3	<10	···
"Pure"	*L* 45	<100	···
"Pure"	*L* 19	···	···
"Pure"	*L* 63	(Recrystallized)	···

[a] Letter designates method of preparation—*L* is lab-grown, *D* is impurity diffused into Harshaw crystal, *H* is as-received Harshaw crystal.

[10] A. B. Lidiard, *Bristol Conference Report on Defects in Crystalline Solids, 1954* (The Physical Society, London, 1955), p. 283.

[11] H. C. Kremers, Ind. Eng. Chem. **32**, 1478 (1940).

[12] Colloidal Graphite in Isopropanol, No. 154, Acheson Colloid Company, Port Huron, Michigan; "Flexible Silver Coating," No. 16, Hanovia Chemical and Manufacturing Company, East Newark, New Jersey.

to the large faces of the samples and the edges were then cleaved away. In this way, the chance that surplus paint might produce short circuits was eliminated. Silver paint was used to fasten the samples to the high-voltage electrode. The electrometer input lead, a 5-mil gold wire, was also attached to the sample by the use of silver paint.

The amount of divalent impurity was determined by spectrographic analysis where the samples were compared to standards containing weighed amounts of each impurity. The sample itself, rather than another part of the ingot, was usually used for the analysis. Results of the analysis are given in column 3, Table I.

The rejection of the impurity from the solidifying sodium chloride decreased as the ionic radius of the impurity increased. This behavior was established by comparing the known amounts of impurities in the melt to the results of spectrographic analysis of the samples taken from the bottom of the ingot. The results appear in column 4 of Table I. It is noteworthy that Cd^{++} was rejected about three times as strongly as Ca^{++}.

III. EXPERIMENTAL METHODS

The sample container was basically a stainless steel Dewar. Ceramic feed-through insulators were used for the electrical connections, including the electrometer input lead. Vacuum or very dry nitrogen prevented surface conduction due to moisture having condensed on the sides of the sample. Spurious dielectric polarizations were eliminated by having the minimal amount of electric insulation near the electrometer input and in the region of changing electric fields. For example, quartz sample insulators initially near the electrometer input gave polarization effects comparable to those in doped sodium chloride crystals. Accordingly, the equipment was altered to eliminate such quartz insulators.

A vacuum tube input electrometer, Keithley Model 610, measured the transient current. This instrument has a minimum feedback factor of 100. The primary benefit of this feedback was a greatly enhanced response speed. The feedback also reduced the input impedance by one hundred times; therefore, there was much less danger of poor insulators partially shunting the electrometer input. An adjustable two section *R-C* filtering network reduced the sixty cycle and microphonic noise appearing in the electrometer output.

The dielectric polarization was observed as a decreasing transient current immediately after the application of a constant electric field. A Tektronix Model 645 oscilloscope and a camera were used to record the transient currents. For most polarization measurements 250 volts were applied to the sample and the grid short removed 0.1 sec later. This time delay allows the lattice displacement polarization to reach equilibrium before current measurements are commenced, and thus avoids overloading the electrometer. The application of the voltage also triggered the scope sweep circuit. A second trace was made with the electric field in the opposite direction. Use of the average of the magnitudes of these two traces eliminated most errors due to electrometer grid current, switching transients, and imbalances in the dc amplifiers. Three to five pictures were taken at each temperature, with sweep times in the range 0.5 to 50 sec. For each sweep time the optimum setting of feedback, grid resistor, *R-C* filtering network, and scope sensitivity were used. The equipment was capable of detecting about 10^{16} dipoles/cm^3 assuming the dipoles to be associated nearest-neighbor vacancy impurity complexes.

The polarization measurements were usually made over the range of $-80°$ to $+25°$C. A one-liter liquid nitrogen chamber above the sample provided cooling. Constant temperatures were maintained by adjusting the current through a cylindrical resistance heater which surrounded the sample. The temperature was measured by a copper-constantan thermocouple located in the ceramic insulator on which the sample was mounted, at a distance 0.5 mm below the sample. The temperature measurements are accurate to $\pm 0.2°$C.

The magnitude of the entire polarization vs time curve was the same regardless of whether it was determined upon application or upon removal of the applied field. Using electric fields with magnitudes in the ratio 4:1 also produced a proportionate change in the polarization current. Such linearity of current with field is indicative of a bulk polarization phenomenon, and not a result of blocking of the ionic flow at the electrodes.[13]

The normal ionic conductivity is very small below 0°C, and, therefore, did not interfere with polarization measurements. Between 0° and +25°C, the small conductivity could be subtracted from the time-dependent polarization effects, or alternately, the measurement could be taken of the current flowing upon removal of the polarizing voltage.

IV. EXPERIMENTAL RESULTS

A typical curve of polarization current vs time for a doped sodium chloride crystal is shown in Fig. 2, which is a composite of oscilloscope traces with four sweep rates. From this figure it is clear that the observable polarization at $-29°$C is made up of two parts. In the first part, the initial polarization current is shown decreasing exponentially in time for almost two decades in the current. This portion of the decay will be referred to as the "fast polarization." The inverse slope of this initial portion is defined as the relaxation time, τ, for the fast polarization. The second part of the curve, called the "slow polarization," is defined as the residual current after subtracting off the fast polarization; this part can not be fitted to a single exponential decay.

At somewhat lower temperatures, evidence for the

[13] G. Jaffe, Ann. Physik **217**, 249 (1933).

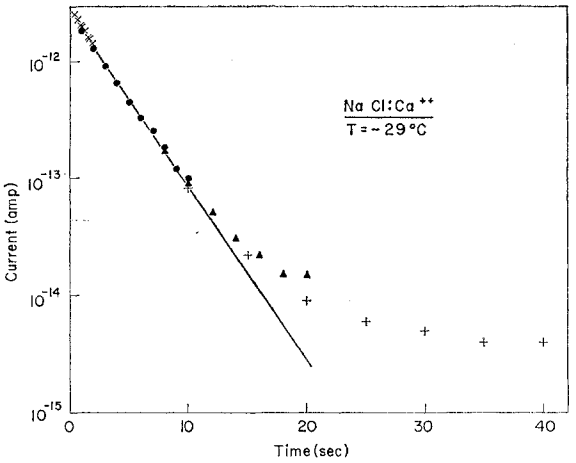

FIG. 2. A typical result from the measurement of the polarization current flowing after the application of a field of 6.8×10^3 volts/cm at zero time. This graph is a composite of data from photographs taken at four different oscilloscope sweep rates, and denoted by the four different symbols. The inverse slope of the initial exponential decay is defined as the fast polarization time, τ.

existence of a polarization current with a time constant even shorter than that associated with the fast polarization was observed in most cases. Figure 3 illustrates this effect for the cases of NaCl crystals doped with Mn^{++} and Zn^{++}. The magnitude of this "very fast polarization" is a small fraction of the normally observed "fast polarization." This figure also indicates the difficulty in obtaining accurate data on the magnitude and time constant of the very fast polarization for such impurities as Mn^{++} because of the need for subtracting the large fast polarization effect. The clearest case of a very fast polarization is observed in Zn^{++}-doped crystals, where the polarization resulting from this very rapidly decaying current was estimated to be over one-third of the magnitude of the fast polarization. The slow polarization, as defined above, is not apparent in Fig. 3 because its relaxation rate is greatly diminished at this low temperature. As the temperature is decreased the decay times associated with both the fast and very fast polarizations decrease in approximately the same ratio. The polarization current was occasionally checked at temperatures as low as -100°C; evidence for the existence of further relaxations was not found.

The magnitudes of these relaxations are dependent upon the presence of divalent impurity ions. In fact, the fast and very fast polarizations were not detected in an as-received Harshaw crystal. In this same Harshaw crystal, the slow polarization was present, although its magnitude was relatively small as compared to a doped crystal. The polarization currents in the laboratory-grown "pure" crystals are also smaller than in the case of the doped crystals.

Results from polarization measurements over the temperature range of 0° to -65°C, show that the time constant of the fast polarization τ, is thermally activated and follows an Arrhenius-type equation (see Fig. 4 and the data designated "Present Work" in Fig. 5). Similar results also were obtained for NaCl:Cd^{++} and Zn^{++}.

In order to determine whether the fast polarization is due to the relaxation process involving the reorientation of impurity-vacancy complexes under the influence of an electric field, a comparison between relaxation times measured in the present dc experiments and those measured from ac dielectric loss experiments appeared desirable. The most complete ac data are those for the system NaCl:Mn^{++} obtained by Watkins[9] in the megacycle frequency range and by Haven[7] in the kilocycle range. Watkins has presented a method of calculating the relaxation time for the nearest-neighbor complexes from the dielectric loss data. Accordingly, the relaxation times for the fast polarization in the present experiments on Mn^{++}-doped crystals are compared with the relaxation times calculated[14] from Watkins' data, as shown in Fig. 5. The data of Haven are also included. The combined data are represented by the Arrhenius-type equation,

$$\tau^{-1}=A\exp(-\epsilon/kT), \qquad (1)$$

with activation energy $\epsilon=0.680\pm0.010$ ev and fre-

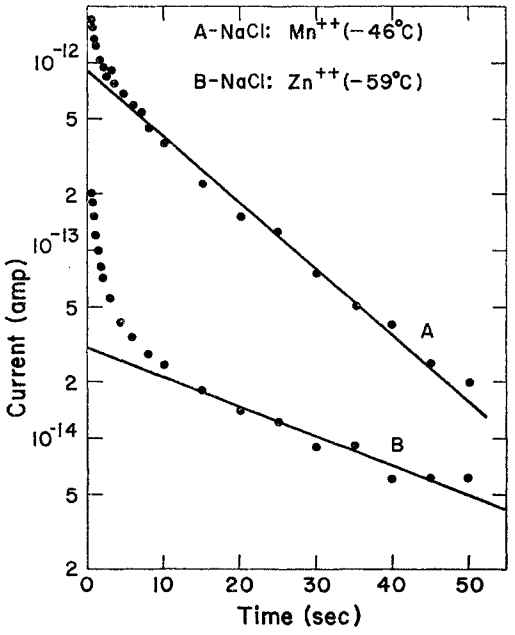

FIG. 3. The polarization current vs time as measured at a relatively low temperature. The straight line is identified as the "fast" polarization current. The presence of a small, very fast polarization current at a time below 10 sec is to be noted. Only in the case of NaCl:Zn^{++} was this "very fast" polarization current of sufficient magnitude to be measured accurately.

[14] The value of τ as measured by ac methods from the position of the Debye peak has been increased by 22% in order to indicate only the nearest-neighbor relaxation component. The calculation of this correction is given on p. 95, reference 9. From the high-frequency data alone, Watkins had obtained a value of $\epsilon=0.63\pm0.05$ ev.

quency factor A of 9×10^{13} sec^{-1} (to within a factor of 1.5). It should be noted that the range covered is more than nine decades in τ. The straight line of Fig. 5 with these parameters fits both the ac and dc measurements within the experimental error of each. Accordingly, it appears reasonable to conclude that the exponential decay in the dc polarization (for NaCl:Mn^{++}) is due to the relaxation of the impurity-vacancy complex in the n.n. position.

In a similar way, Fig. 5 shows that both the ac and dc data for NaCl:Ca^{++} can be accurately fitted to Eq. (1) by using the same A value as in the case of NaCl:Mn^{++}. The shift in τ then indicates a slightly higher activation energy, 0.702 ± 0.010 ev, as compared to the Mn^{++} doped crystals.

The values of ϵ determined from the slopes of $\log\tau$ vs $1/T$, are tabulated in column 3, Table II, for all the impurities studied. These ϵ values are obtained only from the present data, obtained below 0°C. Also shown in Table II are the values ϵ (constant A) which are calculated by assuming A to be independent of impurity radius. The two activation energies agree within experimental error. Based on the data for the Mn^{++}- and Ca^{++}-doped crystals, and in the absence of high-temperature data for the other impurities, it seems reasonable that the best values of ϵ for all cases are those obtained by taking A as a constant equal to 9×10^{13} sec^{-1}.

The frequency factor for the n.n. relaxation, A, of Eq. (1) is about fifteen times larger than the Debye frequency, 5.9×10^{12} sec^{-1}, for NaCl. According to the theory of Zener[15]:

$$A=l\nu\exp(\Delta S/k), \tag{2}$$

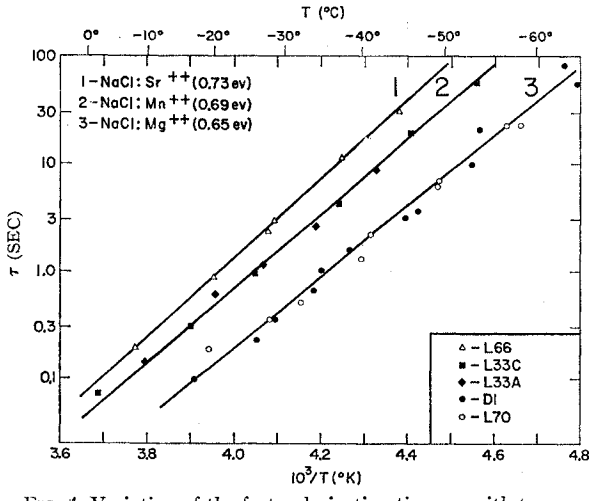

FIG. 4. Variation of the fast polarization time, τ, with temperature for NaCl:Mg^{++}, Mn^{++}, and Sr^{++}. The reproducibility of τ with respect to changes in concentration of a particular impurity ion is illustrated by the comparison of data for different samples. (The time constant has not been corrected to exclude the effects of background impurities. This small correction has been made in Fig. 5, however.)

[15] C. Zener, *Imperfections in Nearly Perfect Crystals* (John Wiley & Sons, Inc., New York, 1952), Chap. 11, p. 289.

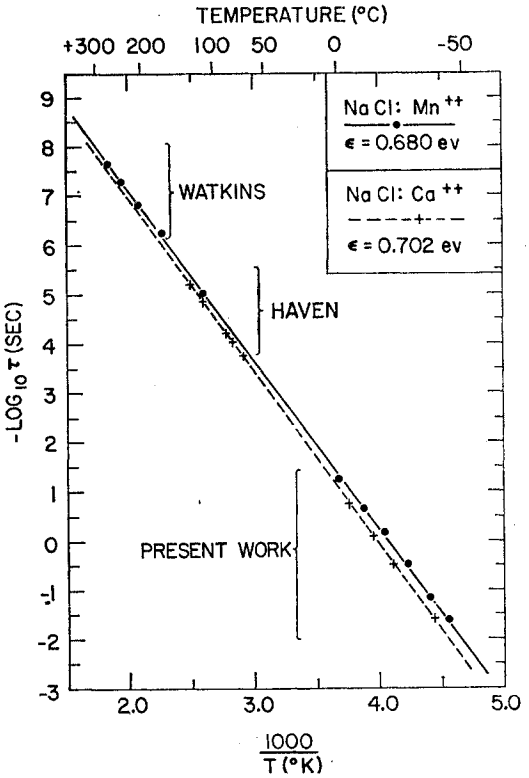

FIG. 5. Variation of relaxation time with absolute temperature for Mn^{++}- and Ca^{++}-doped crystals. These curves show the agreement between the present dc polarization measurements and the earlier ac measurements by Watkins and Haven.

where ΔS is the entropy change when an ion goes from the equilibrium to the saddle point position, ν is an ionic vibrational frequency, and l is the number of similar vacancy jumps, each of which is capable of producing relaxation. The present results give $\Delta S=2.2k$, when ν is set equal to the Debye frequency and l has the value two. Values of this magnitude for ΔS are commonly found in diffusional processes.[15]

The exact magnitude of τ at a given temperature depends upon which impurity is present. In general, the larger the divalent impurity ion, the slower the relaxation. The effect is most evident when the relaxation time is plotted vs ionic radius for a particular temperature. The present results are shown in the upper curve of Fig. 6, where the ionic radii are those given by Pauling.[16] On the right-hand scale, ϵ (constant A) values are shown, as were given in Table II. Figure 6(b) presents the results of Dryden and Meakins[8] obtained by dielectric loss measurements above 0°C on doped KCl crystals. The horizontal scales have been shifted so that the radius of the sodium ion in the

[16] L. Pauling, *Nature of the Chemical Bond* (Cornell University Press, Ithaca, New York, 1945), 2nd ed., p. 346. Other authors have given somewhat different values for the absolute magnitude of ionic radii. However, for the present discussion the relative values of the ionic radii are of primary importance, and these values are not significantly altered by the different procedures used to calculate the ionic radii.

TABLE II. Activation energies and magnitudes of dielectric polarizations measured in NaCl.

Impurity (ionic radius in A)	Sample	ϵ[a][$\log\tau$ vs $1/T$] (ev)	ϵ[constant A][b] (ev)	τ at -35°C[b] (sec)	$j_0T\tau/E$ (°K sec/ohm cm)[b]	Concentration of n.n. dipoles[b] (cm^{-3})	(ppm)	Relative magnitude of slow to fast polarization
Mg (0.65)	*L* 67	...	...	...	$<3\times10^{-14}$	...	...	...
Mg (0.65)	*L* 70	0.65±0.03	0.661	0.85±0.06	2×10^{-13}	...	...	0.6
Mg (0.65)	*D* 1			0.89±0.06	5.6×10^{-13}	...	...	0.2
Zn (0.74)	*L* 68			0.64±0.20	6.9×10^{-14}	6.9×10^{16}	3.1	1.4
Zn (0.74)	*L* 69	0.66±0.13	0.656	0.45±0.25	2.2×10^{-14}	2.2×10^{16}	1	2.6
Zn (0.74)	*D* 3			0.72±0.10	3.9×10^{-14}	3.9×10^{16}	1.8	1.9
Mn (0.80)	*L* 33*A*			2.6 ±0.5	3×10^{-13}	3×10^{17}	14	0.7
Mn (0.80)	*L* 33*B*	0.69±0.03	0.680	2.2 ±0.5	1.9×10^{-13}	1.9×10^{17}	8.6	0.6
Mn (0.80)	*L* 33*C*			2.4 ±0.5	1.14×10^{-13}	1.14×10^{17}	5.2	0.5
Cd (0.97)	*L* 40	0.67±0.03	0.693	4.5 ±0.5	1.7×10^{-13}	1.7×10^{17}	7.7	0.8
Ca (0.99)	*L* 64	0.67±0.03	0.702	6.1 ±0.2	2.8×10^{-13}	2.8×10^{17}	13	0.1
Sr (1.13)	*L* 66	0.73±0.03	0.705	7.2 ±0.2	4.5×10^{-13}	4.5×10^{17}	20	0.07
Harshaw	*H* 3	...	...	...	$<2\times10^{-14}$	$<2\times10^{16}$	<1	...
"Pure"	*L* 45	0.70±0.03	0.702	6.9 ±0.3	1×10^{-13}	1×10^{17}	4.5	...
"Pure"	*L* 19	0.66±0.06	0.698	5.7 ±0.6	1×10^{-13}	1×10^{17}	4.5	...
"Pure"	*L* 63	0.73±0.04	0.703	7.2 ±0.6	8.1×10^{-14}	8.1×10^{16}	3.6	...

[a] ϵ values based upon only the present results (from dc polarization measurements below 0°C).
[b] Concentrations and time constants have been corrected to exclude background impurities in the doped samples. In the Zn^{++}- and Mg^{++}-doped crystals, the background impurity (Ca^{++}) polarization was resolvable, and hence, directly separable. In the other doped crystals, the polarization current characteristic of *L* 45 was subtracted from the current vs time result.

upper graph falls over the radius of the potassium ion in the lower graph. The comparison of the two plots will be discussed in the next section.

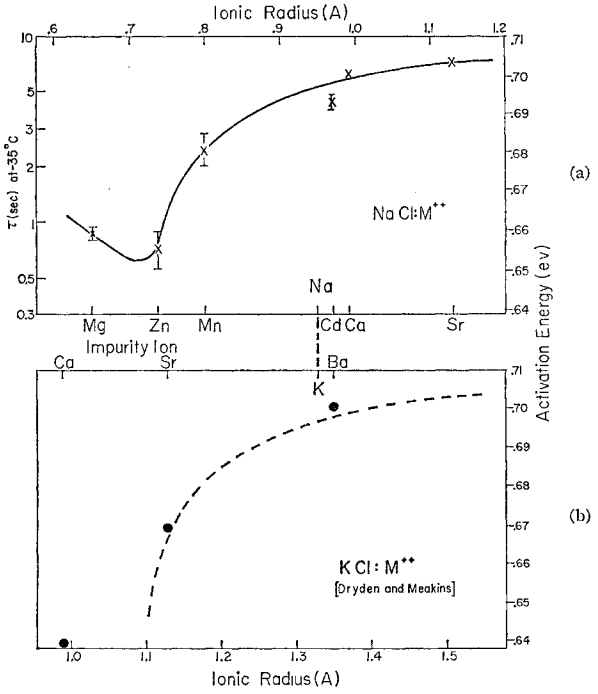

FIG. 6. (a) (Upper curve) The relaxation time, τ, at -35°C vs the ionic radius of the impurity ion for doped NaCl crystals from the present measurements. The right-hand column lists the activation energies calculated from the τ values assuming that the frequency factors remain constant [see Eq. (1)]. (It is shown in Sec. V, however, that the ev scale is probably not applicable to NaCl:Mg^{++}.) (b) (Lower curve) Similar data of Dryden and Meakins for KCl. The two graphs have been aligned by placing the radius of Na^+ over the radius of K^+.

If one knows the nature of the polarizable dipoles contributing to the fast polarization, one can calculate the concentration of such dipoles from the magnitude of the fast polarization current. The agreement between Watkins' results and the present measurements have strongly suggested that the fast polarization is due to nearest-neighbor impurity-vacancy complexes. In Sec. V-A, it will be shown that this interpretation of the fast polarization is also valid for all the other impurities except Mg^{++}, and possibly Zn^{++}. Assuming for now that the nearest-neighbor pairs are responsible for the fast polarization current, and, since the time derivative of the polarization, $P(t)$, is equal to the current density $j(t)$, we obtain for the steady-state polarization, $P(\infty)$,

$$P(\infty)=\int_0^\infty j(t)dt=ae\Delta n, \tag{3}$$

where Δn is the net concentration of the dipoles oriented by the field and ae is the dipole moment of each.

When the magnitude of the current decays exponentially with time constant τ, the following relation may be written

$$P(\infty)=\int_0^\infty j_0e^{-t/\tau}dt=j_0\tau. \tag{4}$$

The net concentration of dipoles oriented by the field, E, is related to the concentration of n.n. impurity-vacancy complexes, N_n:

$$\Delta n=[e^{Eae/kT}-e^{-Eae/kT}]N_n/3\approx\tfrac{1}{3}N_n(2Eae/kT). \tag{5}$$

Combining Eqs. (3), (4), and (5) to eliminate $P(\infty)$ and Δn, gives

$$N_n=3k[j_0T\tau]/2a^2e^2E. \tag{6}$$

Values of $j_0\tau T/E$, obtained experimentally, and the corresponding values of N_n, calculated from Eq. (6), are presented in Table II. It is noteworthy that the fast relaxation usually accounts for only 1–10% of the impurity ions present, as is shown by comparing Tables I and II. For example, about 10 ppm of Mn^{++} dispersed in the NaCl lattice could produce the polarization magnitude observed in crystals containing a total of 200 ppm of Mn^{++} ions. The small magnitude observed can be accounted for if a large portion of the impurity ions are in a precipitated state.

The accuracy of the measurement of each magnitude $j_0T\tau/E$ is $\pm 10\%$. It is, therefore, not possible to verify the T factor in Eq. (6), since T changes by only 20% in the range of these experiments; however, there was no discrepancy noted within the temperature range covered by the present measurements, i.e., the quantity $j_0\tau T/E$ for a given sample was independent of temperature, to within experimental error.

An observable fast polarization ($\tau \approx 6$ sec at $-35°C$) apparently due to calcium ions, is present in the lab-grown "pure" crystals (though not in the Harshaw crystals). The magnitude and time constant can be accounted for by five ppm of Ca^{++} (or Sr^{++}) impurity. Semiquantitative spectroscopic analysis indicates this order of magnitude of Ca^{++} ions present in all lab-grown crystals. This background relaxation is not present in the samples doped by diffusing Zn^{++} or Mg^{++} into Harshaw crystals. The impurity relaxation is, however, present to the same degree in Zn^{++}- and Mg^{++}-doped laboratory-grown samples, the only doped crystals where it is clearly observable. Because the τ values for the fast polarization in Zn^{++}- and Mg^{++}-doped crystals are so much smaller than that of Ca^{++}-doped crystals, the effects of the residual impurity is resolvable and therefore may be excluded. For the remaining (Mn^{++}-, Cd^{++}-, Ca^{++}-, and Sr^{++}-) doped samples, where τ values are close to that of the residual impurity and therefore not resolvable, the time-dependent polarization current due to the residual impurity was subtracted from the measured polarization current. An error in the magnitude of the background polarization would result in an error in the time constant, τ. The effect of a 50% error in background polarization magnitude is included in the estimated accuracy shown in Fig. 6(a).

The slow portion of the polarization curve (see Fig. 2) is not a simple exponential decay, nor can it be resolved into a unique sum of simple exponentials, thus indicating that the appropriate relaxation times are closer together than an order of magnitude. In order to describe the slow polarization, the current density data were fitted with a discrete series of exponentially decaying currents:

$$j(t)=\sum_n j_n \exp(-t/\tau_n). \tag{7}$$

A value for the steady-state polarization after infinite time is found by substituting the above series into Eq. (3) and carrying out the integration:

$$P(\infty)=\sum_n j_n\tau_n. \tag{8}$$

Each τ_n value can now be substituted into Eq. (1) in order to find a corresponding activation energy ϵ. In obtaining these activation energies the frequency factor, A, is assumed to have a value of 1.8×10^{14} sec^{-1}. This value is consistent with the electrical polarization being produced by a vacancy jumping to one of four similar lattice sites instead of two as in the case of nearest-neighbor relaxation, and the same entropy factor as for the n.n. case [see Eq. (2)]. The shape of the slow polarization curve is found to be independent of the amount or type of impurity present. These factors do, however, have an effect upon the over-all magnitude of the slow-polarization curve. As a result of such analysis of the slow polarization it is found that the shortest τ values involved correspond to activation energies of about 0.75 ev, but that there is no indication of an upper limit to the activation energy. Since it is known[17] that a completely free cation vacancy has a jump activation energy of 0.78 ev, it is assumed that components of the slow polarization for which $\epsilon > 0.78$ ev must be due to other causes, such as the effects studied above room temperature by Sutter.[18] Accordingly, in the calculation of the magnitude of the slow polarization, the data were arbitrarily cut off at relaxation times corresponding to $\epsilon = 0.78$ ev. In any case, even if the cutoff used neglects a portion of the relevant (impurity-vacancy complex) polarization, the similarity in shape of the slow polarization curves for various impurities suggests that the results tabulated are at least valuable for comparison of different impurities. Table II, column 8, gives values of the ratio of the magnitude obtained in this way to the magnitude of the fast polarization.

V. DISCUSSION

A. "Fast" and "Very Fast" Polarizations

In NaCl:Mn^{++} and NaCl:Ca^{++} crystals, it was shown that the fast polarization current was due to the same relaxation process as that observed by Watkins and Haven, respectively. In addition, the spin resonance results of Watkins[19] showed that the relaxation process is due to vacancies in the n.n. position of a Mn^{++} impurity ion. There are, however, several types of jumps which can produce the reorientation of an n.n. complex under the influence of an electric field. It is possible to obtain information about the relative importance of each type of jump by considering the variation of relaxation time, τ, with the radius of the impurity ion. The first step is to derive the relation between τ and the individual jump frequencies, while

[17] R. W. Dreyfus and A. S. Nowick (to be published).
[18] P. Sutter, thesis, Yale University, 1959; P. Sutter and A. S. Nowick (to be published).
[19] G. D. Watkins, Phys. Rev. **113**, 79 (1959).

in the second step the changes in these specific jump frequencies with changes in the ionic radius of the impurity ion are roughly determined. Thus, correlations between changes in τ and changes in the ionic radius of the impurity ion can be used to indicate which jump frequencies are predominantly influencing the relaxation rate.

Lidiard[10] expressed the time dependence of the concentrations of vacancies in the various n.n. and n.n.n. positions as functions of the applied electric field and the various relevant ionic jump frequencies, and has provided solutions to these equations for the case of an ac applied field. The equations do not include jumps involving ionic sites farther than $2a$ from the impurity ion. For present purposes the solution of Lidiard's equations under a dc electric field is required. This solution, derived in the Appendix, expresses the polarization, $P(t)$, and current density, $j(t)$, as the sum of two exponential terms, as follows:

$$P(t)\equiv P_1(1-e^{-\lambda_1 t})+P_2(1-e^{-\lambda_2 t}), \tag{9}$$

$$j(t)=dP(t)/dt=P_1\lambda_1 e^{-\lambda_1 t}+P_2\lambda_2 e^{-\lambda_2 t}, \tag{10}$$

where

$$P_1=\frac{4a^2e^2N_iE}{3kT(2+w_4/w_3)(\lambda_1-\lambda_2)}\times[2(w_0+w_4)-\lambda_2(1+w_4/w_3)], \tag{11}$$

$$P_2=\frac{4a^2e^2N_iE}{3kT(2+w_4/w_3)(\lambda_1-\lambda_2)}\times[\lambda_1(1+w_4/w_3)-2(w_0+w_4)], \tag{12}$$

and

$$\lambda_{1,2}=2w_3+w_0+w_4\pm[(w_0+w_4-2w_3)^2+4w_3w_4]^{\frac{1}{2}}, \tag{13}$$

where λ_1 and λ_2 correspond to the $+$ and $-$ signs, respectively. In the above equations:

$$w_0\equiv w_1+w_2,$$

and N_i is equal to the concentration of impurity ions having vacancies occupying n.n. or n.n.n. sites. In these equations, the symbol w_1 designates the jump frequency for interchange between an n.n. sodium ion and an n.n. vacancy (as shown in Fig. 1) in the absence of an applied field. Similarly, w_2 represents the interchange of the divalent impurity ion and an n.n. sodium-ion vacancy, w_3 the motion of an n.n.n. vacancy to an n.n. site, and w_4 that of an n.n. vacancy to an n.n.n. site.

It is also shown in the Appendix that the ac solution of this problem can actually be expressed as the sum of two Debye peaks with relaxation times given by the reciprocals of λ_1 and λ_2.

Returning to the dc solution for the magnitudes and time constants of the polarization, it is clear that, in general, the polarization cannot be separated into purely n.n. and n.n.n. relaxational modes. Rather the solution may be described as two modes coupled together, analogously to the case of coupled vibrational modes. It is noteworthy that $\lambda_1\geq\lambda_2$ under all conditions. For additional insight into the meaning of these solutions for a dc applied field, it is helpful to consider two special cases.

Case I. Simplification of Eqs. (11)–(13) is obtained if the following approximation is valid:

$$w_0\gg 2w_3,w_4. \tag{14}$$

Under these conditions, the parameters characterizing the solution have the values:

$$\lambda_1\approx 2w_0+2w_4, \quad \text{(n.n. relaxation)} \tag{15}$$

$$\lambda_2\approx 4w_3, \quad \text{(n.n.n. relaxation)} \tag{16}$$

$$P_1/P_2\approx w_3/w_4. \tag{17}$$

The latter quantity indicates the relative magnitude of the two relaxations.

The time constants and relative magnitude now have the characteristics of n.n. and n.n.n. relaxations. The quantity $2w_0+2w_4$ is equal to the sum of jump frequencies for all the single jumps of an n.n. vacancy which can change the polarization, while the quantity $4w_3$ is the sum of the jump frequencies for an n.n.n. vacancy. The ratio P_1/P_2 is seen to be equal to the probability of a vacancy occupying each n.n. type site divided by the probability of occupancy for each n.n.n. type site.[10] In summary, if the jump from one n.n. site to another is much faster than any of the other vacancy jumps, the polarization takes on the characteristics of two separate relaxations, simulating a redistribution of n.n. and n.n.n. vacancies, respectively.

Case II. A second approximation also exists which results in the polarization appearing as separate n.n. and n.n.n. relaxations:

$$2w_3\gg w_0,w_4. \tag{18}$$

This assumption means that the jump from an n.n.n. to an n.n. site is the fastest vacancy jump, and thereby also implies that a vacancy occupying an n.n. site is a much more probable situation than one occupying an n.n.n. site. Equations (11)–(13) now have the form:

$$\lambda_1\approx 4w_3+w_4, \quad \text{(n.n.n. relaxation)} \tag{19}$$

$$\lambda_2\approx 2w_0+w_4, \quad \text{(n.n. relaxation)} \tag{20}$$

$$P_1/P_2\approx w_4/4w_3. \tag{21}$$

The relaxation times, λ_1^{-1} and λ_2^{-1}, can now be associated with n.n.n.- and n.n.-type vacancies, respectively, based on essentially the same argument as was given for Case I. The principal distinction is that for Case I, the faster relaxation, λ_1, is the one which involves the relaxation of n.n.-type vacancies, while for Case II, the faster relaxation is that of the n.n.n.-type vacancies. It should be noted, however, that for Case II the ratio P_1/P_2 is small, so that the faster relaxation is not the major effect.

In general, as long as w_4 is relatively small (as is valid for both Cases I and II), one of the relaxation frequencies can be associated with the jumps of n.n.-type vacancies and the other with n.n.n.-type vacancies. When w_4 is larger than either of the other jump frequencies, this division into n.n.- and n.n.n.-type relaxational modes is not evident.

When w_4 is set equal to zero, we have the example, considered often in the previous literature, of only an n.n. relaxation. The polarization then appears as either a single Debye peak or single exponential decay [as was given in the simplified result, Eq. (6)] in the corresponding experiments.

Having obtained expressions for the dependence of the appropriate relaxation times on the various vacancy jump frequencies, we may now proceed with the second step, i.e., to consider how each jump frequency depends on the radius of the impurity ion. Changes in ionic radius of the impurity provide merely a second-order correction to the jump frequency w_1, since it is only the shift of the nearest chlorine ion positions which alters the potential barrier for the jumping of the sodium ion. It seems reasonable that the jump activation energy associated with w_1 should not decrease by more than hundredths of electron volts as the radius of the impurity ion decreases. On the other hand, the magnitude of w_2 will depend very strongly on the radius of the impurity ion, since in this case it is the impurity ion which is doing the jumping. The diffusion experiments of Chemla[20] demonstrated that the activation energy associated with w_2 can decrease by tenths of electron volts when the impurity radius is decreased by 50%. In these experiments, radioactive Zn^{++} and Sr^{++} were used to measure the diffusion coefficient and thereby obtain this information about w_2. The variation of w_1 and w_2 as a function of impurity-ion radius is illustrated qualitatively in Fig. 7(a).

The jump frequencies w_1 and w_2 always appear as the sum, w_0, in the solutions for the time constants and polarization magnitudes given in Eqs. (11)–(13). For impurity ions with radii larger than the radius of Na^+, w_2 should be much less than w_1, which will result in $w_0 \approx w_1$. It seems reasonable that the quantity w_2 should form the major contribution to w_0 only when the radius of the impurity ion becomes significantly (10–15%) smaller than the radius of the alkali metal ions. This changing character of w_0 is illustrated schematically in Fig. 7(b).

An estimate of the variation of w_3 and w_4 with impurity-ion radius must include the effect of the potential energy differences of vacancies in n.n. or n.n.n. positions. The requirement of equilibrium with no applied electric field provides the relation:

$$w_3/w_4 = \exp(\epsilon_{\text{n.n.}} - \epsilon_{\text{n.n.n.}}/kT), \qquad (22)$$

where $\epsilon_{\text{n.n.}}$ and $\epsilon_{\text{n.n.n.}}$ are the binding energies of

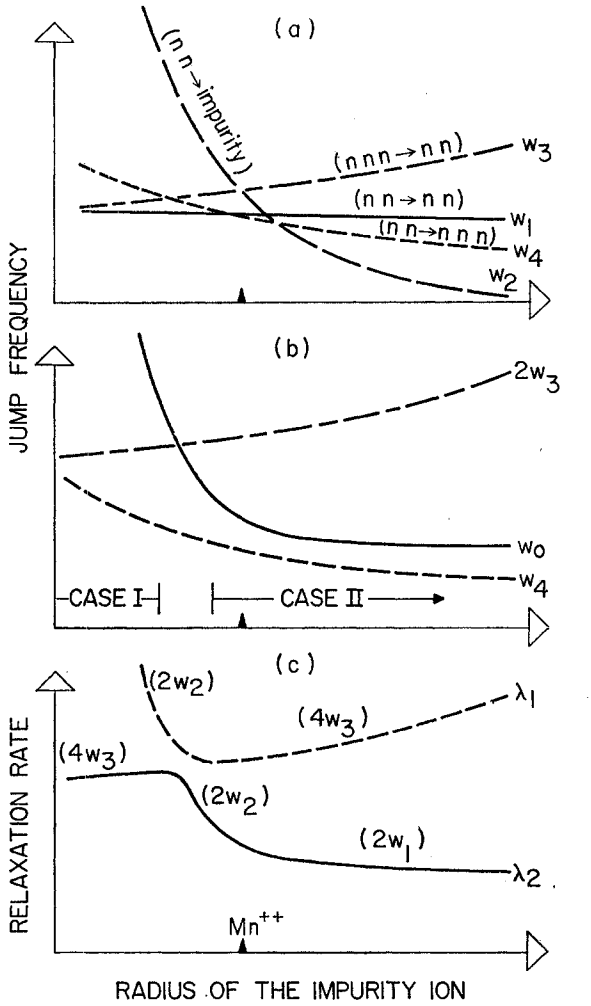

FIG. 7. (a) The anticipated dependence of the individual jump frequencies upon the radius of the impurity ion. The vacancy motion corresponding to each jump frequency is indicated within the parentheses. (b) The relative magnitude of the three jump frequencies which determine the applicability of the approximate solutions for Cases I or II. (c) The dependence of the relaxation rates λ_1 and λ_2 upon the radius of the impurity ion as derived from (a) and (b). The jump frequency which predominates in each range is given in parentheses.

vacancies in the indicated positions. The theoretical calculations of Bassani and Fumi[3] have indicated an increase in the magnitude of $\epsilon_{\text{n.n.}}$ with increasing radius of the impurity ion. In the absence of additional information, the following two assumptions will be made, both of which appear to be reasonable as first approximations: (a) the quantity $\epsilon_{\text{n.n.n.}}$, and (b) the product $w_3 w_4$ should be independent of the radius of the impurity ion. According to (a), the ratio w_3/w_4 is expected to increase with increasing ionic radius, while bringing in assumption (b), shows that w_3 will increase and w_4 will decrease with increasing ionic radius. The variation of w_3 and w_4 with radius should, however, be gradual; there is no reason why they should show the more drastic character of the w_2 variation. Figure 7(a)

[20] M. Chemla, Ann. phys. 1, 959 (1956).

shows, qualitatively, the variation of w_3 and w_4 with ionic radius, based on the above considerations.

As for the relative positions of the curves in Fig. 7(a), we have less information available; the most pertinent information comes from the spin resonance results of Watkins.[9,19] For NaCl:Mn^{++}, Watkins concluded that $\epsilon_{n.n.}-\epsilon_{n.n.n.}=0.034$ ev. At $-35°C$, this implies $w_3=5.3w_4$. This relation, combined with the previous estimates of changes in the ratio w_3/w_4, justifies the assumption that $2w_3\gg w_4$ for all the impurities with radii equal to or greater than Mn^{++}.

The estimate concerning the relative magnitude of $2w_3$ as compared to w_0 for NaCl:Mn^{++} is only obtained by an extrapolation of admittedly scanty available data. Linewidths, as measured by the spin resonance techniques of Watkins,[9] provide information on the n.n. and n.n.n. vacancy jump times. Based on these measurements, Watkins was led to conclusions which may be interpreted in the form: $(4w_3)^{-1}\approx\frac{2}{3}(4w_1+w_2+2w_4)^{-1}$ and $w_2\leq 4w_1$, both at $\sim 250°C$. Under the assumption that all the w's have the same frequency factor, it can be shown from the above data that $5w_0\geq w_3\geq w_0$ for NaCl:Mn^{++} at $-35°C$. For the larger impurity ions the relation presumably becomes $2w_3\gg w_0$. Since $w_3=5.3w_4$, the inequalities:

$$w_0>w_4>w_0/5.3,$$

are implied for the case of NaCl:Mn^{++} at $-35°C$. The above relations are the basis for the positioning of the curves in Figs. 7(a) and 7(b).

Figure 7(b) illustrates how the above evaluation of the jump frequencies separates the relaxations into Cases I and II [defined by Eqs. (14) and (18), respectively], depending upon the impurity-ion radius. For impurity ions larger than Mn^{++}, $2w_3\gg w_0$, w_4; thereby indicating the applicability of Case II. Figure 7(c) shows the corresponding variations of λ_1 and λ_2 given by Eqs. (19) and (20) in the Case II region.

Figure 7(b) illustrates that for impurities with very small radii, the approximations will be valid which indicate the applicability of Case I, viz., $w_0\gg 2w_3$, w_4. Thus, the rapid increase of w_2, for ions smaller than Na^+, has produced a transition from Case II to Case I. Under these conditions, one cannot predict *a priori* whether w_3 or w_4 will be larger; hence, it cannot be predicted whether P_1 or P_2 will represent the larger polarization when Case I applies. Nevertheless, the P_2 polarization now takes on the character of an n.n.n. relaxation effect, as λ_2 becomes equal to $4w_3$. Figure 7(c) shows the changes in both λ_1 and λ_2 with impurity ionic radius. The quantities given in parentheses are the predominant rates in each range. Simple approximate solutions apparently do not exist in the transition region between Cases I and II.

The above predictions concerning the behavior of the relaxation rates with changes in the radius of the impurity ion can now be compared with the observed changes in τ illustrated in Fig. 6. It should be noted that the quantity plotted in Fig. 6 is the relaxation time, while its reciprocal, the relaxation rate, is shown in Fig. 7(c). For the larger impurity ions, a unique relaxation time, τ, is observed and is presumed to be λ_2^{-1}. Also, the observation of a very fast polarization of small magnitude can now be explained in terms of the faster relaxation for which the relaxation rate is λ_1, and which is predominantly an n.n.n. relaxation. The assumption that $2w_3\gg w_0$ for the larger impurity ions thus provides the basis for a direct interpretation of the very fast polarization. Returning to Fig. 6, the quantity τ is found to be almost independent of the ionic radius of the impurity for NaCl:Cd^{++}, Ca^{++}, and Sr^{++}, as predicted for λ_2 in Fig. 7(c) for large impurity ion radii. Furthermore, τ drops rapidly (or τ^{-1} increases rapidly) in going from Cd^{++} to Mn^{++} to Zn^{++}, again in agreement with the predicted increase of λ_2 in Fig. 7(c).

In the case of NaCl:Zn^{++} the very fast polarization has increased in magnitude, so that the polarization shows two distinct relaxational modes. Only the time constant of the larger relaxation (associated with P_2, λ_2) is shown in Fig. 6. The very fast polarization observed at the earlier times is approximately eight times faster and approximately four-tenths in magnitude as compared to the fast polarization. The fact that the λ_1 relaxation now appears to be clearly observable is presumably a result of w_4/w_3 having increased to approximately unity for small impurity ions, and the corresponding increase in the magnitude of P_1/P_2 as shown by Eq. (21). The presence of two relaxations with not too dissimilar time constants and magnitudes in the case of NaCl:Zn^{++} makes it doubtful that the assumptions leading to either Case I or II are fulfilled; it seems, rather, that the case of NaCl:Zn^{++} falls in the transition region.

Finally, Fig. 6 shows a leveling off as we go from Zn^{++} to Mg^{++}. This is in agreement with Fig. 7(c) and indicates that the transition from Case II to Case I has essentially taken place for the Mg^{++}-doped samples. Accordingly, the value plotted in Fig. 6(a) for NaCl:Mg^{++} is $(4w_3)^{-1}$, the relaxation time of the n.n.n. vacancies, not that of the n.n. vacancies.[21] The experimental observation that $P_1\ll P_2$ for NaCl:Mg^{++} then implies that $w_3\ll w_4$ for such a small impurity ion.

Presumably, the data for impurity-doped KCl of Dryden and Meakins, given in Fig. 6(b), indicate a similar interpretation.

Summarizing, comparison of theoretical predictions with the experimentally determined dependence of τ upon the radius of the impurity ion in NaCl crystals leads to the following conclusions: (a) In the case of

[21] The activation energy scale on the right in Fig. 6(a) does not apply to the case of vacancy motion in NaCl:Mg^{++} because of the factor 4 in the relation $\lambda_2\approx 4w_3$. This changed numerical factor results in Fig. 6(a) indicating a value 0.014 too small for ϵ for NaCl:Mg^{++}. In addition, it should be realized that in the case of Mg^{++} doping the activation energy refers to the motion of the n.n.n. vacancies.

Mn^{++}-, Cd^{++}-, Ca^{++}-, or Sr^{++}-doped crystals, the dominant unique polarization represents an n.n.-type relaxation; (b) for large impurity ions (Cd^{++}, Ca^{++}, Sr^{++}) the impurity-vacancy reorientation involves the sodium ion jumping between n.n. sites; (c) in the case of impurity ions with radii significantly smaller than the radius of the alkali metal ion, the jumping of the impurity ion into the n.n. vacancy can distinctly enhance the rate of n.n. relaxation; (d) the experimental results for NaCl:Mg^{++} are interpretable as due to complexes in which vacancies predominantly occupy n.n.n. sites with respect to the impurity ion; (e) the rate of jumping from an n.n.n. site to an n.n. site (w_3) appears to be greater than the rate of jumping of an n.n. vacancy to another n.n. site (w_1) for all the impurities studied.

B. "Slow Polarization"

As already mentioned, bound vacancies can occupy sites at distances greater than the n.n.n. sodium-ion site. The probability of occupancy is usually small since the Coulomb attraction of the impurity energetically favors the nearer sites. The effect of the Coulomb attraction is somewhat compensated for by the large number of available sites at greater distances, and the fact that the polarization-per-dipole is proportional to the square of the dipole moment. Calculations based on Coulomb energies for the more distant sites have indicated that finite polarization contributions can be expected from sites up to $4a$ from the impurity ion.

Since the two relaxational modes, P_1 and P_2, predicted from Lidiard's theory have already been accounted for by the fast and very fast polarizations, the effect of more distant vacancies can only be to add additional exponential decay terms in the solution for the polarization current. A convenient notation for the remaining (slow) polarization is $P_{>2}$. An accurate calculation of the magnitudes and time constants of higher than n.n.n. relaxations is difficult to use because of the uncertainties in the appropriate binding energies and jump times. Some qualitative statements can, however, be made about the solutions: (a) For a given divalent impurity, the magnitude of the slow polarization, $P_{>2}$, will be proportional to the concentration of the impurity-vacancy complexes present. (b) Since only jumps which involve reorientation of the complex are considered, the jump time of the more distant relaxations should approach three times the jump time (in a random direction) of a free vacancy. (c) The relative magnitudes of the more distant relaxations will depend primarily upon the n.n. binding energy, since the binding energies of vacancies at distances greater than $2a$ will be essentially independent of the size of the impurity ion while the n.n. binding energy is strongly dependent on impurity size.

The above characteristics of a slow polarization attributable to bound vacancies in relatively distant sites appear to agree with the experimentally observed behavior of the slow polarization. The magnitude of the slow polarization is found to be proportional to the magnitude of the fast polarization for each impurity ion. The latter quantity is considered to be a measure of the concentration of impurity-vacancy complexes present. Also, in the measurements for NaCl:Mg^{++}, Zn^{++}, the magnitude of both the fast and slow polarizations could be correspondingly reduced by slowly cooling the samples through the 200° to 100°C range. It is believed that this treatment should increase the degree of impurity precipitation and hence decrease the concentration of isolated impurity-vacancy complexes.

The activation energy for motion ranges upward from about 0.75 ev. As was mentioned previously, this value is in general agreement with the 0.78-ev activation energy for motion of a free Na^+ ion vacancy.

The magnitude of the slow polarization relative to the fast polarization increases the smaller the radius of the impurity ion, as shown in the last column of Table II, with the exception of Mg^{++}. It has already been shown that for those impurities which fall into the range of applicability of Case II [see Fig. 7(b)], the fast polarization (with magnitude P_2) is proportional to the concentration of n.n. vacancies. On the other hand, for the case of NaCl:Mg^{++}, it was concluded that Case I applies and the fast polarization represents the n.n.n. relaxation effect. Accordingly, the ratio of the slow to fast polarization magnitudes given in Table II have a different theoretical significance, depending on which of the approximations is valid. For Case II, it has the significance of the relative contribution of distant (>n.n.n.) relaxations to that of the n.n. relaxation. This ratio is therefore, plotted in Fig. 8 for all the impurities except Mg^{++}. (The case of Zn^{++} may be regarded as somewhat questionable too,

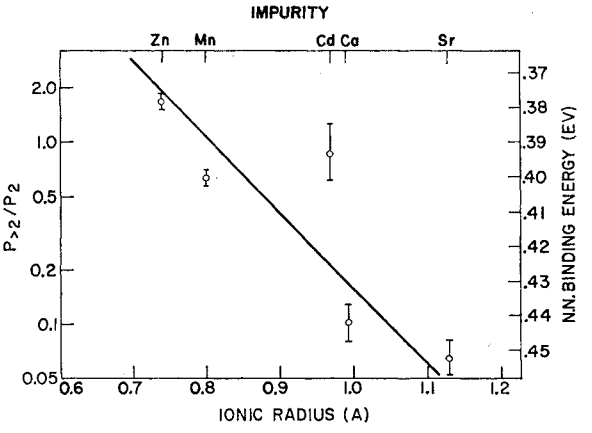

FIG. 8. The relative magnitude of the polarization for dipoles farther than n.n.n. ($P_{>2}$) to that of the n.n. relaxation (P_2) as a function of ionic radius of the impurity ion. The nearest-neighbor binding energies on the right are based on Watkins' value of ~0.4 ev for NaCl:Mn^{++}.

since it has been concluded that this is not clearly Case II, but falls in the transition range.)

A decrease in n.n. binding energy with a decrease in impurity radius is expected on the basis of theoretical[3] results. The reduced n.n. binding energy allows more of the vacancies to be at distances greater than $2a$ and thus the relative magnitude of the slow polarization should be increased. Binding energies are shown on the right in Fig. 8. These values are calculated by assuming the value of 0.4 ev for NaCl:Mn^{++}, as was approximately obtained by Watkins[19] from electron spin resonance results, and comparing the relative magnitude of the slow polarization for NaCl crystals containing other impurities to that of NaCl:Mn^{++}. The results should be taken only as a general indication of the n.n. binding energies.

For crystals other than NaCl:Mg^{++}, $P_{>2}/P_2$ gives the relative magnitude of distant relaxations (>n.n.n.) to that of the n.n. relaxation. For Mg-doped crystals, on the other hand,

$$[\text{Relative magnitude of slow to n.n. relaxation}] = P_{>2}/P_1 > P_{>2}/P_2.$$

Thus, the last ratio, which is plotted in Fig. 8 for the larger ions is anticipated to be too small. A comparison of the last column in Table II and Fig. 8, shows that, indeed, the data for NaCl:Mg^{++} lie well below an extrapolation of the points for the larger impurity ions. It, therefore, appears that not only the results of relaxation time measurements [Fig. 6(a)] but also the results for $P_{>2}/P_2$ support the concept that the major relaxation observed in NaCl:Mg^{++} is of the n.n.n. type.

No conclusive explanation has been found for the differences between Ca^{++}- and Cd^{++}-doped crystals. The differences are noted to occur not only in the fast relaxation time (Fig. 6) and slow relaxation magnitude (Fig. 8), but also in the rejection ratios given in Table I. It appears that in all cases Cd^{++} behaves as if it had a smaller radius than that given in tables of ionic radii.

VI. CONCLUSIONS

The increased resolution possible with dc polarization techniques applied below room temperature, has established a distinct fast polarization interpretable (except for NaCl:Mg^{++}) as a nearest neighbor type relaxation. In some cases (Zn^{++}, Mg^{++}) a distinct n.n.n. relaxation has also been observed. A distribution of slow polarizations, has been identified as due to relaxations involving vacancies at more distant sites. The latter blend into a still slower polarization, similar to the phenomena studied by Sutter[18] above room temperature.

ACKNOWLEDGMENTS

The author is grateful to A. S. Nowick for his guidance and encouragement throughout the course of this work, and to F. G. Fumi and G. D. Watkins for many helpful discussions. The samples were prepared by K. W. Asai, and the spectroscopic analysis was carried out by D. P. Cameron and J. C. Webber.

APPENDIX. POLARIZATION CURRENT FOR A dc APPLIED FIELD

Lidiard[22] expressed the time dependence of the concentrations of vacancies in n.n. and n.n.n. positions as functions of the instantaneous electric field and the field-free atomic jump frequencies, and has provided solutions for the case of an ac applied field. For present purposes, these equations are solved for the dc case (i.e., static applied field E along the $+x$ axis). The equations will not be repeated here, but for ease of reference, the present notation is the same as Lidiard's notation. The impurity ion position is in the plane $x=0$. The quantities N_a, N_b, and N_c are then concentrations of vacancies at each of the four n.n. sites located in the planes $x=+a$, $x=0$, and $x=-a$, respectively. Similarly M_a and M_c are the concentrations of vacancies on each of the n.n.n. sites located at $x=+2a$ and $x=-2a$, respectively, and the concentration M_b refers to the four n.n.n. sites located in the plane of the impurity ion.

The homogeneity of Lidiard's six equations and the symmetry requirements with respect to the applied electric field, indicate that the solution is of the form:

$$N_a=N-n_1(1-e^{-\lambda_1 t})-n_2(1-e^{-\lambda_2 t}), \quad \text{(A1)}$$

$$N_b=N, \quad \text{(A2)}$$

$$N_c=N+n_1(1-e^{-\lambda_1 t})+n_2(1-e^{-\lambda_2 t}), \quad \text{(A3)}$$

$$M_a=M-m_1(1-e^{-\lambda_1 t})-m_2(1-e^{-\lambda_2 t}), \quad \text{(A4)}$$

$$M_b=M, \quad \text{(A5)}$$

$$M_c=M+m_1(1-e^{-\lambda_1 t})+m_2(1-e^{-\lambda_2 t}). \quad \text{(A6)}$$

Here the quantities N and M are the zero-field equilibrium concentrations of vacancies at n.n. and n.n.n. sites, respectively.

It was found necessary to use a solution involving two time constants, thereby confirming the result (using group theory) of Haven and van Santen[23] that two modes of relaxation are operating.

The constants in Eqs. (A1–A6) are determined by substituting the above relations into the differential equations given by Lidiard. The results for the reciprocal time constants λ_1 and λ_2 obtained in this way are given in Eq. (13) of the text. The following relationships are found for the relative magnitudes of the exponential relaxation terms:

$$n_i/m_i=(4w_3-\lambda_i)/4w_4, \quad (i=1, 2). \quad \text{(A7)}$$

Auxiliary conditions are obtained from the equilibrium distributions which exist, first, for zero electric

[22] See reference 10; Eqs. (*A*1*a*)–(*A*1*f*), pp. 294 and 295.
[23] Y. Haven and J. H. van Santen, Nuovo cimento **7**, 605 (1958).

field, and then in the presence of the applied field, E:

$$M/N=w_4/w_3, \tag{A8}$$

$$n_1+n_2=(aeE/kT)N, \tag{A9}$$

$$m_1+m_2=(2aeE/kT)M. \tag{A10}$$

The solutions for m_1, m_2, n_1, and n_2 are obtained by combining Eqs. (A7–A10).

The net polarization, $P(t)$, is derived from the concentration of each type of dipole multiplied by the appropriate dipole moment:

$$P(t)=2ea(M_c-M_a)+ea(4N_c-4N_a). \tag{A11}$$

Substituting into Eq. (A11) the results of the above solution, one obtains

$$P(t)=\frac{4a^2e^2NE[(w_0-2w_3+w_4)^2+4w_3w_4]^{-\frac{1}{2}}}{kT}\times\{(1-e^{-\lambda_1 t})[2(w_0+w_4)-\lambda_2(1+w_4/w_3)]+(1-e^{-\lambda_2 t})[\lambda_1(1+w_4/w_3)-2(w_0+w_4)]\}. \tag{A12}$$

At the relatively low temperature involved in the present experiments, the impurity ions can be assumed to be essentially all in an associated state. The equilibrium concentration of vacancies at each position is then related to the concentration of impurity ions, N_i:

$$N_i=12N+6M=6N(2+w_4/w_3). \tag{A13}$$

By using Eqs. (9), (13), and (A13), the relation (A12) can be separated into the two polarization magnitudes given in Eqs. (11) and (12) of the text.

In view of the fact that the dc solution consists of two exponential terms, one may be led to wonder why Lidiard did not express the ac solution as the sum of two Debye peaks. In fact, Lidiard stated that only by introducing the effect of vacancy sites more distant than n.n.n. could one obtain a second Debye peak. A re-examination of the ac solution, however, shows that it can be expressed as two Debye peaks. By algebraic manipulation of Eqs. (A4) and (A6) of Lidiard's paper, which represent the ac solution to the problem, they can be put in a form analogous to that given in Eq. (A12) of the present paper, as follows:

$$P(\omega)=\frac{4a^2e^2NE_0e^{-i\omega t}}{kT}[(w_0-2w_3+w_4)^2+4w_3w_4]^{-\frac{1}{2}}\times\left\{\frac{2(w_0+w_4)-\lambda_2(1+w_4/w_3)}{(1-i\omega/\lambda_1)}+\frac{\lambda_1(1+w_4/w_3)-2(w_0+w_4)}{(1-i\omega/\lambda_2)}\right\}, \tag{A14}$$

where $\omega/2\pi$ is the frequency of the applied voltage. The loss angle, δ, is given by

$$\tan\delta=\frac{32\pi a^2e^2N}{\epsilon kT(\lambda_1-\lambda_2)}\left\{\frac{2(w_0+w_4)-\lambda_2(1+w_4/w_3)}{(\lambda_1/\omega+\omega/\lambda_1)}+\frac{\lambda_1(1+w_4/w_3)-2(w_0+w_4)}{(\lambda_2/\omega+\omega/\lambda_2)}\right\}, \tag{A15}$$

which is simply the sum of two Debye peaks with relaxation times λ_1^{-1} and λ_2^{-1}, respectively.

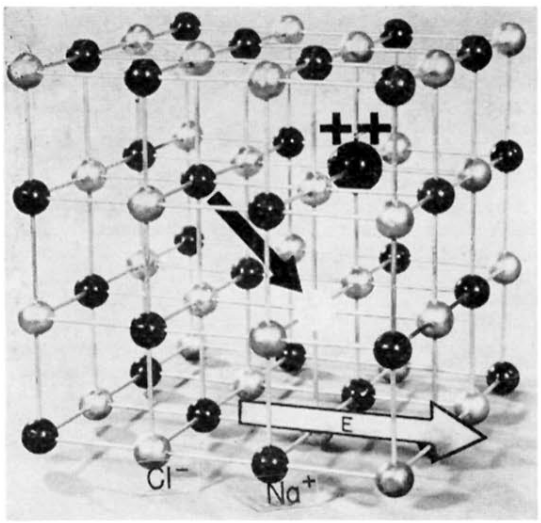

FIG. 1. Model of a lattice in which a vacancy (in white) is the nearest neighbor (n.n.) of a doubly charged metallic impurity ion. The interchange of an n.n. sodium ion with the n.n. vacancy, which would be favored by the applied electric field, **E**, is shown.